Proceedings of Fifth International Conference on **Enhanced, Compact and Ultra-Compact Heat Exchangers: Science, Engineering and Technology**, Eds. R.K. Shah, M. Ishizuka, T.M. Rudy, and V.V. Wadekar, Engineering Conferences International, Hoboken, NJ, USA, September 2005.

CHE2005 - 23

Role of Numerical Modeling in Compact Heat Exchanger Analysis

P. Nithiarasu

School of Engineering, University of Wales Swansea, Swansea SA2 8PP, UK; P.Nithiarasu@swansea.ac.uk

ABSTRACT

In this article some numerical modeling procedures of compact heat exchangers are discussed. A simple system analysis, originated from the early finite element methods, is discussed first. The full scale CFD modeling approach follows the system analysis. Prominence is given to various currently available turbulent flow modeling techniques for fluid flow and heat transfer in compact heat exchangers. Recent developments in turbulence modeling approaches and their potential applications in compact heat exchanger analysis are also discussed. Some example problems are also presented to discuss these modeling procedures.

INTRODUCTION

An effective design for a heat exchanger is the one which maximizes the heat transfer while reducing the power expended. Increase in surface area, which is the primary feature of many compact heat exchangers, invariably increases the heat transfer. However, this also increases the power expended and cost. There are several books and papers published on the basic design procedures of heat exchangers (Kays and London, 1964) based on experimental and theoretical studies of the past. However, some challenges of heat exchanger design will remain with us for fore-seeable future. This is due to the fact that the heat exchanger designs need to adopt itself to the ever growing process, power and aerospace industries. As these industries grow, more precise design of heat exchangers and suitable materials become crucial. The reduction in space occupied, better performance and cost effective designs would be future objectives of the heat exchanger industry.

In recent times, the traditional design procedures using the experimental data and analytical based approaches have been complemented by the numerical based approaches. The reasons for the change in the trend are due to two reasons. The first reason is the ever growing computing power and the second is the availability of better software tools. For instance the unstructured mesh generation of complex flow domains and solution to turbulent flow in these domains are becoming increasingly common in the literature. Thus, in this article computational analysis of heat exchanger surfaces, which eventually can lead to an optimal design, is discussed.

The major objective of any numerical modeling approach in heat exchangers is to relate the heat transferred to the total power expended. This may be achieved via several paths. However, the common goal of any analysis will be to reach an optimal design.

The design process starts with an initial problem design. Here human instinct (common sense) and previous experience helps to come up with a basic idea and the numerical calculations help in the refinement of the initial design to create an optimal one. Once an initial design is available the next stage is the simplification and this step depends a great deal on the tools available. If available numerical tools are comprehensive then the simplification to the initial design will me minimal. However, with any numerical tool one has to make sure that the problem is not over simplified to an extent to lose the accuracy of physics. The third step is the input data generation suitable for the numerical tool employed. Here the geometrical modeling, mesh arrangement (or generation) and necessary boundary and initial conditions will be part of

the input data generation. The fourth step is the numerical solution. If the objective is only to increase the heat transfer rate then one would be interested in a detailed temperature distribution. However, a comprehensive analysis should produce the relation between heat transfer and power expended bearing in mind the complex shapes involved in the design and cost. The fifth step involves the analysis of the results and determining whether or not the design is satisfactory. If not the problem is redefined based on the results obtained in the forth step. The redefining can be automated via optimization techniques by prescribing the objective functions for simple geometries. However, even for a simple geometry the number of parameters can be many.

In this article we concentrate on the numerical modeling of flow and heat transfer in compact heat exchanger channels. The following section briefly describes a system analysis. In the latter sections, computational fluid dynamics approach is discussed in detail. Some example problems are also presented as and when required.

SYSTEM ANALYSIS

The performance of a heat exchanger can be calculated in terms of its effectiveness for a given condition. In order to determine the effectiveness of a heat exchanger, we have to calculate the outlet temperatures of both the hot fluid and the cooling fluid for the given inlet temperatures. The overall heat transfer coefficient may be a constant or could vary along the heat exchanger.

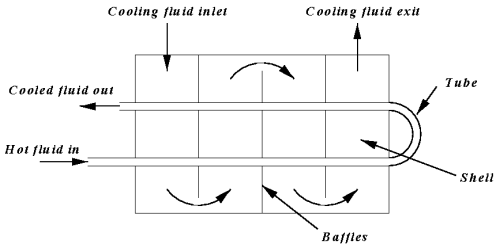

Figure 1 Schematic diagram of a shell and tube heat exchanger

For the purpose of illustration let us consider a shell and tube heat exchanger as shown in Figure 1 (Holman, 1989; Incropera and Dewitt, 1990). In this type of heat exchanger, the hot fluid flows through the tube and the tube is passed through the shell. The cooling fluid is pumped into the shell and thus the hot fluid in the tube is cooled.

Let us divide the given heat exchanger into eight cells as shown in Figure 2 (Lewis et al., 2005; Ravikumar et al., 1984). It is assumed that both the hot and cold fluids will travel through the cell at least once. Let the overall heat transfer coefficient be U and the surface area of the tubes be A. These are assumed to be constant throughout the heat exchanger within each element (cell). Let us assume that the hot and cold fluid temperatures vary linearly along the flow.

Now, the heat leaving node 1 and entering element 1 (Figure 1(b)) is

$$Q_1 = W_1 T_1 \tag{1}$$

where W_1 is ρc_p times volume flow rate. The heat leaving element 1 and entering node 2 is (The energy balance is considered with respect to the element. Heat entering is taken as being positive and leaving the element is taken as negative)

$$Q_2 = W_1 T_1 - UA(T_{1,2} - T_{11,12}) \tag{2}$$

where $T_{1,2} = 0.5\ (T_1 + T_2)$ and $T_{11,12} = 0.5\ (T_{11} + T_{12})$

Similarly, the heat leaving node 11 and entering element 1 is

$$Q_{11} = W_2 T_{11} \tag{3}$$

and the heat leaving element 1 and entering node 12 is

$$Q_{12} = W_2 T_{11} - UA(T_{11,12} - T_{1,2}) \tag{4}$$

In this example the heat transfer between the fluids is given by $UA\ (T_{11,12} - T_{1,2})$ whereas some other models use $UA(T_{12} - T_{11,12})$. The assumption in the present model is more logical in view of the continuous variation (linear in our case) of the temperature difference between the hot and cold fluids.

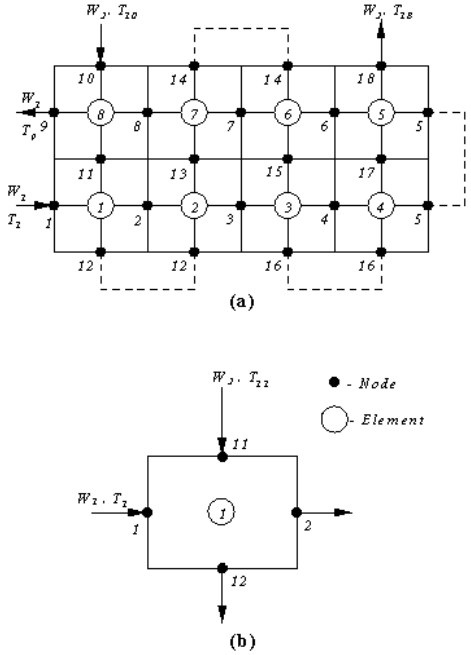

Figure 2 System analysis of shell and tube heat exchanger

Equations (1) – (4) can be combined and recast in matrix form to give the element characteristics, i.e.,

$$\begin{bmatrix} W_1 & 0 & 0 & 0 \\ W_1 - C & -C & C & C \\ 0 & 0 & W_2 & 0 \\ C & C & W_2 - C & C \end{bmatrix} \begin{Bmatrix} T_1 \\ T_2 \\ T_3 \\ T_4 \end{Bmatrix} = \begin{Bmatrix} Q_1 \\ -Q_2 \\ Q_{11} \\ -Q_{12} \end{Bmatrix} \quad (5)$$

where $C = UA/2$.

Assembly of the element characteristics for elements 1 to 8 will results in the global stiffness matrix in which Q_1, and Q_{10} are known (in other words T_1, and T_{10} are known).

The solution of the remaining equations will give the temperature distribution for both the fluids i.e., T_2, T_3, T_4, T_5, T_6, T_7, T_8 and T_9 for the incoming hot fluid and T_{11}, T_{12}, T_{13}, T_{14}, T_{15}, T_{16}, T_{17} and T_{18} for the coolant.

With the known exit temperatures T_9 and T_{18}, the effectiveness of the heat exchanger can be calculated.

Though simple, the system analysis may not give very accurate results due to the simplifying assumptions used. Also, generalizing this method to complex situations is difficult. In what follows, we discuss the more general analysis of computational fluid dynamics methods.

COMPUTATIONAL FLUID DYNAMICS STUDY

The computational fluid dynamics study has been the subject of recent interest to many heat exchanger analysts due to the vast computational resources available nowadays and development in numerical solution techniques and mesh generation in the last thirty years (Amon, 1995; Amon and Mikic, 1991; Atkinson, 1998; Fabbri, 2000; Ciofalo, 1996; Groll and Mertz, 1997; Islamoglu and Parmaksizoglu, 2004; Sunden, 1999; Tafti et al., 1999; Wang et al., 1996). There are several commercial softwares available in addition to a number of research codes.

It is often necessary for a researcher to develop his own software or routines to model special cases of heat exchangers. The fluid dynamics and heat transport in a heat exchanger is governed by the incompressible Navier-Stokes equations. The Navier-Stokes equations consist of conservation of mass, momentum and energy. In the incompressible flow context the energy equation becomes a transport equation for temperature. The Navier-Stokes equations may be summarised in a compact form as

Continuity

$$\frac{\partial u_i}{\partial x_i} = 0 \quad (5)$$

Momentum

$$\frac{\partial u_i}{\partial t} + u_i \frac{\partial u_i}{\partial x_i} = -\frac{1}{\rho}\frac{\partial p}{\partial x_i} + \nu\left(\frac{\partial^2 u_i}{\partial^2 x_i^2}\right) + g_i \quad (6)$$

Energy

$$\frac{\partial T}{\partial t} + u_i \frac{\partial T}{\partial x_i} = \alpha\left(\frac{\partial^2 T}{\partial x_i^2}\right) \quad (7)$$

In the above equations suffixes i and j indicate the directions. u_i are the velocity components in x_i (or x_j) directions, t is the time, ρ is the density, ν is the kinematic viscosity, T is the temperature and α is the thermal diffusivity.

The above equations are valid for any incompressible flow problems including flows with turbulence. However, molecular level turbulence needs extremely large computing power and extremely expensive at operating Reynolds numbers of compact heat exchangers. Thus, to tackle the turbulence phenomena generally Large Eddy Simulation (LES) or Reynolds Averaged Navier-Stokes

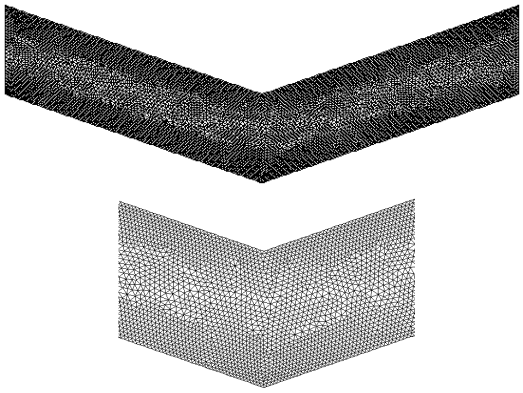

Figure 3 Laminar flow and heat transfer in a corrugated channel. Unstructured mesh

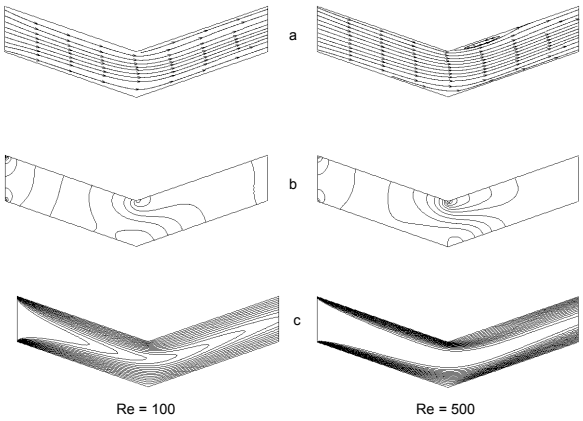

Figure 4 Laminar flow and heat transfer in a corrugated heat exchanger channel (a) Stream traces (b) Pressure and (c) Temperature

(RANS) equations are commonly employed. It is also common nowadays to see researchers using a combination of LES and RANS approaches to model turbulence. Both these modeling techniques are briefly discussed in the following sub-section. However, laminar flow and heat transfer can be solved without any change to the Equations (5) – (7) on reasonable size meshes such as the one shown in Figure 3. Figure 4 shows the stream traces, pressure and temperature contours at Reynolds numbers 100 and 500. A small recirculation is observed at Re = 500 immediately after the middle top turn. As expected thermal boundary layer got thinner as the Reynolds number was increased from 100 to 500. Pressure contours obtained are generally smooth showing that the solution procedure used is stable. These laminar results are generated using the CBS scheme and the finite element spatial discrtization (Nithiarasu, 2003; Nithiarasu et al., 2004; Nithiarasu et al., 2005; Zienkiewicz et al., 2005).

At laminar speeds most of the numerical schemes develop little difficulties on relatively course meshes. However, at moderate and high Reynolds numbers this is not true. At moderate Reynolds numbers, which are the operating Reynolds numbers of most of the compact heat exchangers, turbulence sets in and it will be difficult to resolve these using reasonable meshes such as the one shown in Figure 3. Also, higher order schemes will be necessary even if finer meshes are employed. To overcome these difficulties the Reynolds Averaged Navier-Stokes (RANS) equations are widely employed in analyzing flow through compact heat exchanger geometries.

TURBULENCE MODELLING

RANS Models

For turbulent flow computations, Reynolds averaged Navier-Stokes equations of motion are written in conservation form as follows

Mean continuity

$$\frac{\partial \bar{u}_i}{\partial x_i} = 0 \tag{8}$$

Mean momentum

$$\frac{\partial \bar{u}_i}{\partial t} + \bar{u}_i \frac{\partial \bar{u}_i}{\partial x_i} = -\frac{1}{\rho}\frac{\partial p}{\partial x_i} + \nu\left(\frac{\partial^2 \bar{u}_i}{\partial x_i^2}\right) + \frac{\partial \tau_{ij}^R}{\partial x_i} + g_i \tag{9}$$

where $\bar{u}_i$ are the mean velocity components, τ^R_{ij} are the turbulent Reynolds stresses. The standard linear model for Reynolds stresses (Boussinesq's assumption) is

$$\tau_{ij}^R = -\overline{u_i u_j} = \nu_T\left(\frac{\partial \bar{u}_i}{\partial x_j} + \frac{\partial \bar{u}_j}{\partial x_i}\right) \tag{10}$$

In the above equation, ν_T is the turbulent eddy viscosity. It is clear from the time averaged Navier-Stokes equations (8) – (10) that the additional variable to be determined is the turbulent eddy viscosity. The objective of all RANS models is to determine this. The non-linear

RANS models are developed by assuming a non-linear relation between the Reynolds stresses and strain rate.

κ-l Model (One Equation Model)

In this model the turbulent eddy viscosity is determined from a mixing length and turbulent kinetic energy as

$$\nu_T = c_\mu^{1/4} \kappa^{1/2} l_m \tag{11}$$

where c_μ is a constant equal to 0.09, κ is the turbulent kinetic energy and l_m is the mixing length. The mixing length l_m is related to the length scale of the turbulence L as

$$l_m = \left(\frac{c_\mu'}{C_D} \right)^{1/4} L \tag{12}$$

where C_D and c_μ' are constants.

The model transport equation for turbulent kinetic energy is

$$\frac{\partial \kappa}{\partial t} + u_i \frac{\partial \kappa}{\partial x_i} = \frac{\partial}{\partial x_i}\left(\nu + \frac{\nu_T}{\sigma_\kappa} \right) \frac{\partial \kappa}{\partial x_i} + \tau_{ij}^R \frac{\partial u_i}{\partial x_j} - \varepsilon \tag{13}$$

where σ_κ is the diffusion Prandtl number for turbulent kinetic energy. The dissipation, ε, is modelled as

$$\varepsilon = C_D \frac{\kappa^{3/2}}{L} \tag{14}$$

Near solid walls, the Reynolds number tends to be zero and the highest mean velocity gradient occurs at the solid boundary. Thus, the one equation model has to be used in conjunction with empirical wall functions, i.e, ν_T is multiplied by damping function $f_v = 1\text{-}e^{-0.160R\kappa}$ and ε is divided by $f_b = 1\text{-}e^{-0.263R\kappa}$, where $R_\kappa = \sqrt{\kappa} y/\nu$, with y being the near wall distance. The constants are $\sigma_\kappa = 1$ and $C_D = 1.0$.

SA Model (One Equation Model)

The Spalart-Allmaras (SA) (Spalart and Allmaras, 1992) model was first introduced for aerospace applications and currently being adopted for incompressible flow calculations. The SA model is another one equation model, which employs a single scalar equation and several constants to model turbulence. The scalar equation is

$$\frac{\partial \hat{\nu}}{\partial t} + u_i \frac{\partial \hat{\nu}}{\partial x_i} = c_{b1} \hat{S} \hat{\nu} + \frac{1}{\sigma}\left[\frac{\partial}{\partial x_i}(\nu + \hat{\nu}) \frac{\partial \hat{\nu}}{\partial x_i} + c_{b2} \left(\frac{\partial \hat{\nu}}{\partial x_i} \right)^2 \right] - c_{w1} f_w \left[\frac{\hat{\nu}}{y} \right]^2 \tag{15}$$

where

$$\hat{S} = S + (\hat{\nu} / k^2 y^2) f_{v2}$$

here,

$$f_{v2} = 1 - X/(1 + X f_{v1})$$

In the above equation S is the magnitude of vorticity. The eddy viscosity is calculated as

$$\nu_T = \hat{\nu} f_{v1}$$

where

$$f_{v1} = X^3 / (X^3 + {c_{v1}}^3)$$
$$X = \hat{\nu} / \nu$$

The parameter f_w is given as

$$f_w = g\left[\frac{1 + c_{w3}^6}{g^6 + c_{w3}^3} \right]^{1/6}$$

where

$$g = r + c_{w2}(r^6 - r)$$

with

$$r = \frac{\hat{\nu}}{\hat{S} k^2 y^2}$$

The constants are $c_{b1} = 0.1355$, $\sigma = 2/3$, $c_{b2} = 0.622$, $k = 0.41$, $c_{w1} = c_{b1}/k^2 + (1 + c_{b2})/\sigma$, $c_{w2} = 0.3$, $c_{w3} = 2$ and $c_{v1} = 7.1$.

Standard κ-ε Model

In this model, the transport equation for κ is the same as that in the one-equation model (Equation 13). The second transport equation for calculating the isotropic turbulence energy dissipation rate ε is

$$\frac{\partial \varepsilon}{\partial t} + u_i \frac{\partial \varepsilon}{\partial x_i} = \frac{\partial}{\partial x_i}\left(\nu + \frac{\nu_T}{\sigma_\varepsilon}\right)\frac{\partial \varepsilon}{\partial x_i} + C_{\varepsilon 1}\frac{\varepsilon}{\kappa}\tau_{ij}^R \frac{\partial u_i}{\partial x_j} - C_{\varepsilon 2}\frac{\varepsilon^2}{\kappa} \quad (16)$$

where $C_{\varepsilon 1}$ is equal to 1.44, $C_{\varepsilon 2}$ is equal to 1.92 and σ_ε is the diffusion Prandtl number for isotropic turbulence energy dissipation rate and equal to 1.3. These constants are proposed by Jones and Launder (1972). In addition, ν_T is evaluated by

$$\nu_T = c_\mu \frac{\kappa^2}{\varepsilon} \quad (17)$$

For near-wall treatments, modifications to the source terms of ε equation are needed in the near-wall region. Multiplying the coefficients c_μ, $C_{\varepsilon 1}$ and $C_{\varepsilon 2}$, by the turbulence damping functions f_μ, $f_{\varepsilon 1}$ and $f_{\varepsilon 2}$ appropriate low Reynolds number status near the walls is achieved. These functions are suggested by many and we employ the ones suggested by Lam and Bremhorst (1981) for steady flows. They are

$$f_\mu = (1 - e^{-0.0165 R_K})^2 \left(1 + \frac{20.5}{R_t}\right)$$

$$f_{\varepsilon 1} = 1 + \left(\frac{0.05}{f_\mu}\right)^3$$

and

$$f_{\varepsilon 2} = 1 - e^{-R_t^2}$$

where $R_t = \kappa^2/\nu\varepsilon$

The constants are $C_\mu = 0.09$, $\sigma_\kappa = 1.0$, $\sigma_\varepsilon = 1.3$, $C_{\varepsilon 1} = 1.4$ and $C_{\varepsilon 2} = 1.8$.

TURBULENT ENERGY EQUATION

The temperature equation for a turbulent heat transfer problem is written as

$$\frac{\partial T}{\partial t} + u_i \frac{\partial T}{\partial x_i} = \alpha\left(\frac{\partial^2 T}{\partial x_i^2} + \frac{\nu_T}{\sigma_T}\frac{\partial^2 T}{\partial x_i^2}\right) \quad (18)$$

where σ_T is the turbulent Prandtl number (around unity).

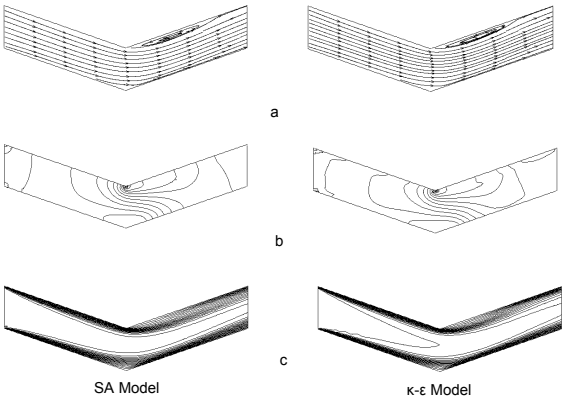

Figure 5 Turbulent flow and heat transfer in a corrugated heat exchanger channel. Comparison of SA model and κ-ε model results at Re = 1000. (a) Stream traces (b) Pressure and (c) Temperature

It is very common to see variations in results obtained by different turbulence models. In Figure 5 the results from two turbulence models for flow through a corrugated channel are shown. As seen, there are minor differences visible between the two results. It is generally known that two equation models are better than one equation models. However, two equation models are more expensive than one–equation models. Among various one equation models used in the literature, SA model seem to give better results (Nithiarasu and Liu, 2005).

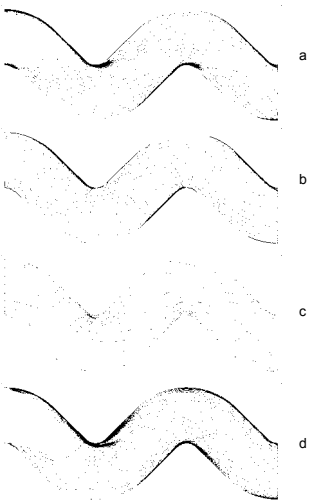

Figure 6 Flow through a smooth corrugated channel at Re = 8280. (a) u_1 velocity (b) u_2 velocity (c) Pressure (d) Turbulent kinetic energy. κ-l model.

Figure 6 shows the results generated for a turbulent flow in a smooth corrugated channel using the *κ-l* model.

ADVANCED TURBULENCE MODELLING

Large Eddy Simulation

The idea of LES is developed based on splitting large scale motions from small scales using a filtering operation such as

$$\overline{\phi}(x) = \int_{\Omega} \phi(x')G(x,x')dx'$$

If the variables of the the incompressible Newtonian equations are subjected to the above filtering operation, we get

$$\frac{\partial \overline{u}_i}{\partial x_i} = 0 \tag{19}$$

and

$$\frac{\partial \overline{u}_i}{\partial t} + \overline{u}_i \frac{\partial \overline{u}_i}{\partial x_i} = -\frac{1}{\rho}\frac{\partial p}{\partial x_i} + \nu\left(\frac{\partial^2 \overline{u}_i}{\partial^2 x_i^2}\right) + \frac{\partial \tau_{ij}^{SGS}}{\partial x_i} + g_i \tag{20}$$

where

$$\tau_{ij}^{SGS} = \overline{u}_i\overline{u}_j - \overline{u_i u_j} \tag{21}$$

τ_{ij}^{SGS} in the above equation is generally modeled using various sub-grid scale (SGS) models. The standard SGS models (Smagorinsky, 1963), dynamic models (Germano, 1992) and non-linear models are a few to mention. It is a vast area of research and difficult to cover all the theory behind these models in a research article. For the sake of completeness, we provide the standard SGS model below. The SGS stress of Equation (21) is identical to Equation (10). However, the eddy viscosity is modeled differently here.

Standard SGS Model

The eddy viscosity here is defined as

$$\nu_T = (C\Delta)^2 \overline{\omega} \tag{22}$$

The most widely used eddy-viscosity model was proposed by the meteorologist Smagorinsky (Smagorinsky, 1963). Smagorinsky was simulating a two-layer quasigeotrophic model in order to represent large (synoptic) scale atmospheric motions. He introduced an eddy viscosity that was supposed to model three-dimensional turbulence with approximately three-dimensional (3D) Kolmogorov $\kappa^{-5/3}$ cascade in the subgrid scales.

In Smagorinsky's model, a sort of mixing-length assumption is made, in which the eddy viscosity is assumed to be proportional to the subgrid scale characteristic length Δ and to a characteristic turbulent velocity based on the second invariant of the filtered field deformation tensor (i.e. strain-rate tensor). In other words, the well-known Smagorinsky's model, where the SGS time scaling ω in Equation (22) is set as the magnitude of the local resolved strain-rate tensor, namely

$$\overline{\omega} = |\overline{S}| = \left(2S_{ij}S_{ij}\right)^{1/2} \tag{23}$$

The constant $C = C_s = 0.1 - 0.18$ is commonly employed. The characteristic length Δ is calculated as

$$\Delta = f(\Delta x_1, \Delta x_2, \Delta x_3)^{1/2}$$

where x_1,x_2 and x_3 are the coordinate directions. Despite increasing interest in developing more advanced subgrid scale stress models, Smagorinsky's model is still successfully used.

Hybrid Methods

Though lesser number of equations is solved in LES than RANS models, the number of mesh points needed in LES calculations is much larger than RANS calculations. To avoid excessive computing requirement of LES, a new family of turbulence modeling technique has been recently proposed (Spalart et al., 1997, Constantinescu et al., 2003). In this method, a RANS model is employed near the walls and LES is employed away from the wall. These types of models are constructed easily. For instance, if we replace the shortest distance to the wall, *y* in SA model by the following relation we get a simple hybrid model.

$$\tilde{y} = \min(y, C_{DES}\Delta) \tag{24}$$

with $\Delta = \max(\Delta x_1, \Delta x_2, \Delta x_3)$. In Equation (24) C_{DES} is a constant (around 0.65), which varies depending on the problem solved. The subscript *DES* indicates 'Detached Eddy Simulation'. Equation (24) clearly shows that RANS equations are used near the walls and LES is used away from the walls.

NUMERICAL SOLUTION

In order to achieve numerical solution to a particular problem of interest, one has to write the above equations in discrete form, both in space and time. These procedures are discussed briefly in the following sub sections.

Temporal Discretization

Dicretization of the time term in the governing equations are referred to as 'temporal discretization'. The common and simple time discretization employed is based on the finite difference approach. Several options are available to discretize the time term. Backward, forward and central difference schemes are some of them.

Spatial Discretization

The two major spatial discretization procedures used in practical applications are finite volume and finite element methods (Hirsch, 1989, Zienkiewicz and Taylor, 2000; Lewis et al., 2004). Both the methods are flexible to be employed on unstructured meshes and widely used in computational fluid dynamics calculations. The vertex centered finite volume method and linear finite element methods are very similar.

MESH GENERATION

Both structured and unstructured meshes are commonly employed in the compact heat exchanger analysis. Though accurate, structured meshes are not easy to generate for complex geometries often encountered in compact heat exchangers. The unstructured meshes are generally easy to generate (Figure 7) but need more number of nodes to achieve the same accuracy of a structured mesh. Also, it is necessary to have a suitable discretization method for unstructured meshes. Obviously the meshes should be refined in the region where high gradients are expected. If the high gradient region is not known, adaptive mesh generation could be used (Nithiarasu and Zienkiewicz, 2000; Nithiarasu, 2002).

When the turbulence models are employed, structured meshes close to walls may give a better accuracy. In such situations, a hybrid mesh may be employed. The hybrid meshes are generated by growing surface normal from solid surfaces and placing structured layers by dividing the normals. One typical example is shown in Figure 8. Here, as seen, the mesh is structured close to the solid wall and unstructured away from the wall. Thus, this mesh may be able to capture near wall turbulence better than a purely unstructured mesh.

DETERMINATION OF HEAT EXCHANGER PERFORMANCE FACTORS

The two important quantities of interest in heat exchanger applications are the rate of heat transfer (Nusselt number) and the flow resistance offered by a surface (drag). Often j and f factors are calculated to estimate the heat exchanger performance. These factors are functions of Nusselt number and pressure drop. In this section a brief summary of how to calculate these quantities is given.

Nusselt Number

The Nusslet number is derived as follows. Let as assume that a hot surface is cooled by a cold fluid stream. The heat from the hot surface, which is maintained at a constant temperature, is diffused through a boundary layer and convected away by the cold stream. The Nusselt number relation for this situation may be derived from Newtons law of cooling as

$$Nu = -\left(\frac{\partial T}{\partial n}\right)^{*} \tag{25}$$

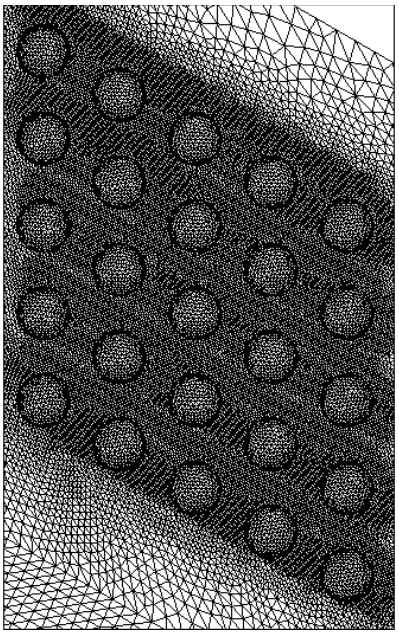

Figure 7 Unstructured surface mesh over a surface with sphereical heat sources.

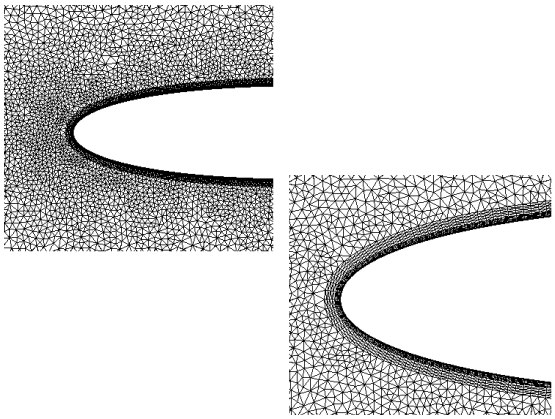

Figure 8 Hybrid meshes.

It should be observed that the local Nusselt number is equal to the local, non-dimensional, normal temperature gradient. The above definition of the Nusselt number is valid for any heat transfer problem as long as the surface temperature is constant, or a reference wall temperature is known. However, for prescribed heat flux conditions a different approach is required to derive the Nuselt number. In such a situation the Nusselt number may be calculated as

$$Nu = \left(\frac{1}{T_w - T_f} \right)^* \tag{26}$$

The equation is simpler than that derived for a constant wall temperature and is limited to the calculation of local non-dimensional wall temperatures (assuming T_f is constant).

Pressure Drop

Pressure drop is directly obtained from a numerical solution if the primitive variable formulation is employed. If stream function-vorticity formulation is employed, extra pos-processing is necessary to determine the pressure drop.

TRANSIENT SOLUTION

All real turbulent flow are transient flows. However, the time averaged turbulent flow equations average all quantities over time. The transient solutions can still be obtained using RANS models with some limitations. For many problems of compact exchangers, either transient evaluation is important or no steady state solution exists. With appropriate time discretization accurate time dependent solutions can be obtained. Figure 9 shows solutions at Re = 1200 at different non-dimensional times. As seen the there is no steady state exist for this problem at this Reynolds number.

MORE RESULTS

Heat Transfer in a Corrugated Channel

Figure 10 shows a corrugated geometry channel of a compact heat exchanger. One portion of the channel is considered for analysis as shown in Figure 10 (bottom). The inlet of the channel is assumed to have a uniform velocity and a temperature lower than the wall temperature. The no-slip conditions are assumed to prevail on the solid surfaces. The width of the channel is taken as the characteristic dimension of the problem and the Reynolds number is defined based on this. The SA model is used in all the calculations.

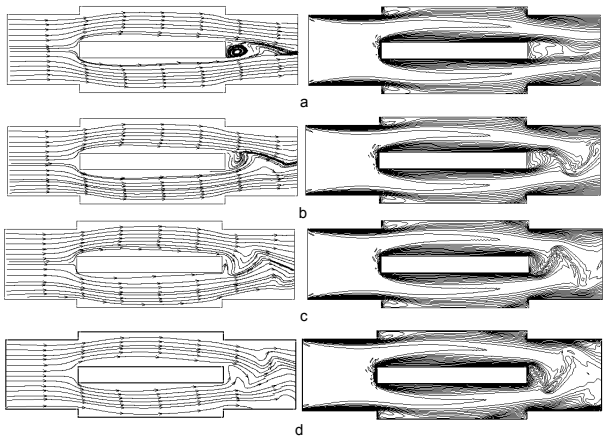

Figure 9 Transient flow and temperature distribution in a offset strip fin heat exchanger (a) t = 0.4 (b) t = 0.6 (c) t = 0.6 (d) = 0.8

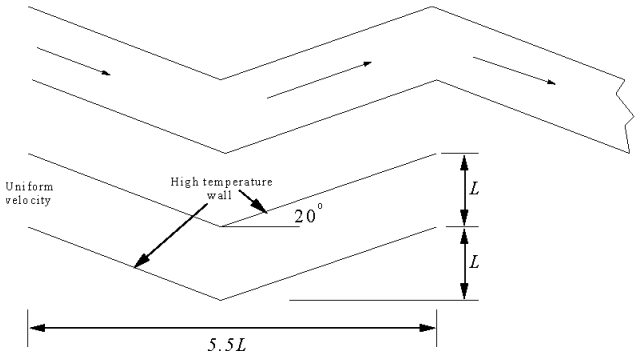

Figure 10 Corrugated channel of a compact heat exchanger. Geometry and boundary conditions

Figures 4 shows the stream traces, temperature and pressure contours at low Reynolds number of 100 and 500. As seen no secondary vortices are seen at Re = 100. However, at Re = 500 a secondary vortex appear immediately after the top corner. At Re = 1000 this vortex size increases (Figure 5). However at higher Reynolds numbers the size of this vortex is reduced as shown in Figure 11. Also at Re = 2000 and 5000, an additional small vortex appear close to the bottom corner.

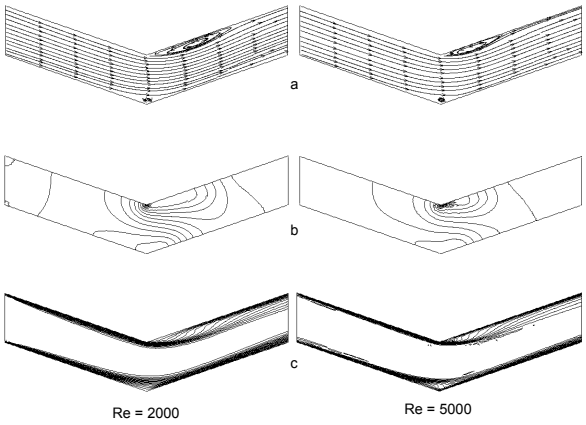

Figure 11 Flow and heat transfer in a corrugated channel at moderate Reynolds numbers. SA model results (a) Stream traces (b) Pressure (c) Temperature

Pressure contours are consistently smooth showing that the numerical scheme used is stable (CBS scheme). The temperature contours indicate appearance of thinner thermal boundary layers as the Reynolds number is increased. This indicates increase in rate of heat transfer as expected.

Figure 12 shows the local Nusselt number distribution at two Reynolds numbers on both solid walls. In both cases and walls, the peak Nusselt number is obtained close to the leading edges. The Nusselt number drops along the top wall towards the turn in the wall. Close to the turn the Nusselt number goes up but drops suddenly immediately after the turn due to the slow flow and recirculation here. Along the bottom wall the Nusselt number decreases towards the turn but increases sharply after the turn due to increased mass flux close to this wall.

The average Nusselt number and pressure drop variations with Reynolds number are shown in Figure 13. As expected the Nusselt number increases with Reynolds numbers on both walls. The value is almost identical on both walls to a Reynolds number of 1000. Beyond Re = 1000, the average Nusselt number on the top wall is higher than at the bottom wall. The Nusselt number variation with Reynolds number shows a non-linear pattern. The non-dimensional pressure drop ($p/\rho u_\infty^2$) reduces as the Reynolds number if increased. The rate of reduction decreases as the Reynolds number is increased.

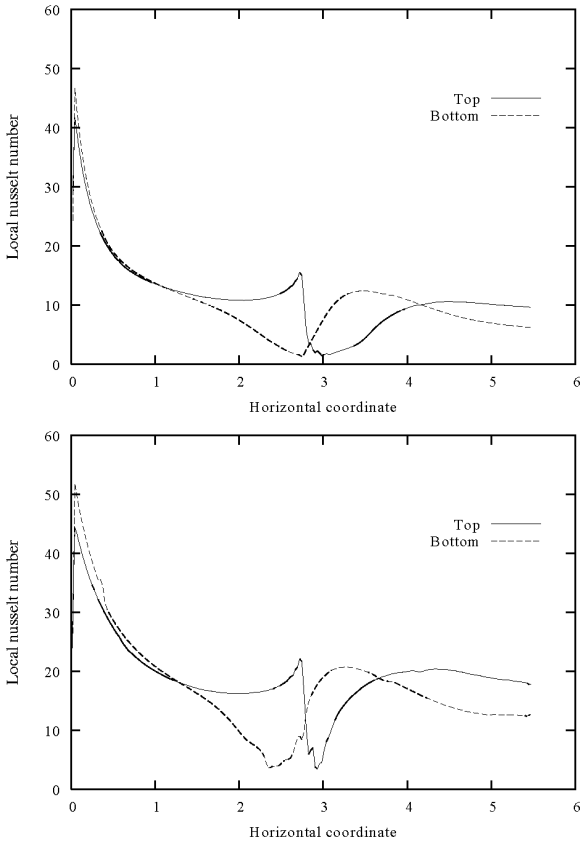

Figure 12 Flow and heat transfer in a corrugated channel at moderate Reynolds numbers. Local Nusselt number distribution at Re = 2000 (top) and Re = 5000 (bottom).

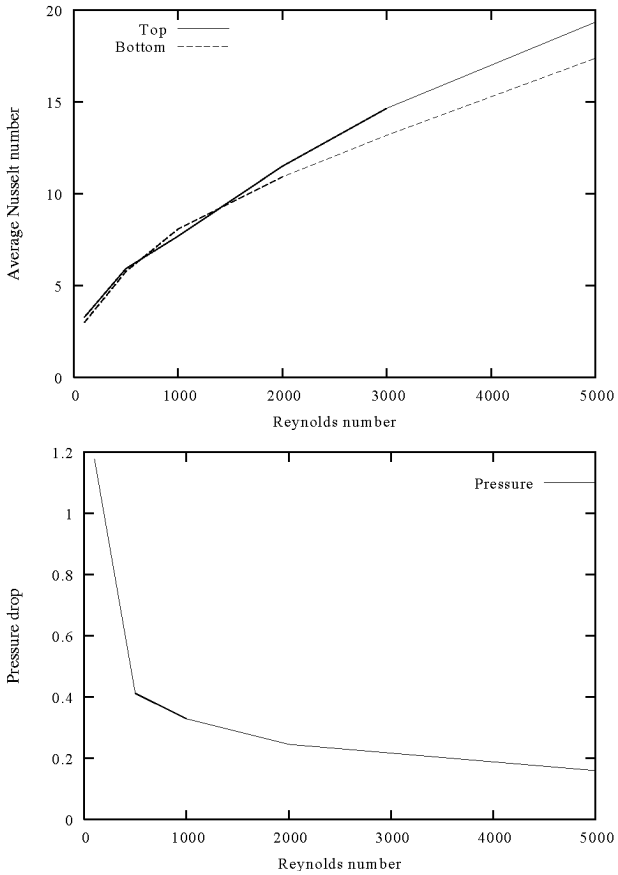

Figure 13 Flow and heat transfer in a corrugated channel at moderate Reynolds numbers. Average Nusselt number (top) and pressure drop (bottom)

CONCLUSIONS

This article presented an overview of numerical modelling approaches employed in the compact heat exchanger analysis. Special attention was given to various turbulence modeling approaches. Some problems and their results are also presented using some of the turbulence modeling approaches. Many recently developed turbulence modeling approaches are yet to be popular among the heat exchanger community. For example, Detached Eddy Simulation can potentially benefit compact heat exchanger analysis. As the demand for more and more precise analysis increases, it will be necessary for many researchers to adopt more advanced fluid dynamics modeling techniques.

REFERENCES

Amon CH, Spectral element-Fourier method for unsteady conjugate heat transfer in complex geometry flows, *Journal of Thermophysics and Heat Transfer*, 9, 247 - 253, 1995.

Amon CH and Mikic BB, Spectral element simulations of unsteady forced convective heat transfer application to compact heat exchanger geometries, *Numerical Heat Transfer Part A - Applications*, 19, 1 - 19, 1991.

Atkinson KN, Drakulic R, Heikal MR and Cowell TA, Two- and three-dimensional numerical models of flow and heat transfer over louvred fin arrays in compact heat exchangers, International *Journal of Heat and Mass Transfer*,41, 4063 - , 1998.

Fabbri G, Heat transfer optimisation in corrugated wall channels, International *Journal of Heat and Mass Transfer*, 43, 4299 - 4310, 2000.

Constantinescu G, Chapelet M and Squires, K, Turbulence modeling applied to flow over a sphere, *AIAA Journal*, 41, 1733 – 1742, 2003.

Ciofalo M, Stasiek J and Collins MW, Investigation of flow and heat transfer in corrugated passages. 2. Numerical Simulations, *International Journal of Heat and Mass Transfer*, 39, 165 - 192, 1996.

Germano M, Turbulence: the filtering approach, *J. Fluid Mech*., 238, 325, 1992.

Groll M and Mertz R, Improved evaporation heat transfer surfaces for cost-effective compact heat exchangers for the process industries, *Applied Thermal Engineering*, 17, 685 - 703, 1997.

Hirsch C, *Numerical Computation of Internal and External FLows, Vol 1*, John Wiley, 1989.

Holman JP, *Heat Transfer*, McGraw-Hill, Singapore, 1989.

Incropera FP and Dewitt DP, *Fundamentals of Heat and Mass Transfer*, John Wiley & Sons, New York, 1990.

Islamoglu Y and Parmaksizoglu C, Numerical investigation of convective heat transfer and pressure drop in a corruguated heat exchanger channel, *Applied Thermal Engineering*, 24, 141 - 147, 2004.

Jones WP and Launder BE, The prediction of laminarization with a two-equation model of turbulence, *International Journal of Heat and Mass Transfer*, 15, 301- 314, 1972.

Kays WM and London AL, *Compact Heat Exchangers, McGraw-Hill Book Company*, Ney York, 1964.

Lam CKG, Bremhorst K, A modified form of the κ-ε model for predicting wall turbulence. *Transications of the ASME Journal of Fluids Engineering*,103, 456-460, 1981.

Lewis RW, Nithiarasu PN and Seetharamu KN, *Fundamentals of the finite element method for heat and fluid flow*, Wiley, Chichester, 2004.

Nithiarasu, P.**,** An adaptive remeshing scheme for laminar natural convection problems*, Heat and Mass Transfer*, 38, 243 – 250, 2002

Nithiarasu P, An efficient artificial compressibility (AC) scheme based on the characteristic based split (CBS) method for incompressible flows, *International Journal for Numerical Methods in Engineering*, 56:1815--1845, 2003.

Nithiarasu P, Mathur JS, Weatherill NP and Morgan K. Three-dimensional incompressible flow calculations using the characteristic based split (CBS) scheme. *International Journal for Numerical Methods in Fluids*, 44:1207--1229, 2004.

Nithiarasu, P., Massarotti, N. and Mathur, J.S., Forced convection heat transfer from solder balls on a printed circuit board using the Characteristic Based Split (CBS) scheme, International Journal of Numerical Methods in Heat and Fluid Flow, *International Journal of Numerical Methods in Heat and Fluid Flow*, 15, 73-95, 2005.

Nithiarasu P, and Liu C-B, An explicit Characteristic Based Split (CBS) scheme for incompressible turbulent flows, *Computer Methods in Applied Mechanics and Engineering*, (Accepted, 2005)

Nithiarasu, P. and Zienkiewicz, O.C., `` Adaptive Mesh Generation for Fluid Mechanics Problems", *International Journal for Numerical Methods in Engineering*, 47, 629 - 662, 2000

Ravikumaur SG, Seetharamu KN and Aswatha Narayana PA, Applications of Finite Elements in Heat Exchangers, *Communications in Applied Numerical Methods*, 229--234, 1984.

Smagorinsky J, General circulation experiments with the primitive equations, I Basic experiment, *Monthly Weather Review*, 91 99, 1963.

Spalart PR and Allmaras SR, A one-equation turbulence model for aerodynamic flows, AIAA paper 92-0439, *AIAA 30th Aerospace Sciences Meeting*, 1992.

Spalart PR, Jou WH, Strelets M and Allmaras SR, Cooments on the feasibility of LES for wings, and on a hybrid RANS/LES approach, *Advances in DNS/LES: First SFOSR International Congress on DNS/LES*, edited by C. Liu and Z. Liu, Greyden, Columbus, OH, 1997.

Sunden B, Enhancement of convective heat transfer in rib-roughened rectangular ducts, *Journal of Enhanced Heat Transfer*, 6, 89 - 103, 1999.

Tafti DK, Zhang LW and Wang G, Time-dependent calculation procedure for fully developed and developing flow and heat transfer in louvered fin geometries, *Numerical Heat Transfer Part - A - Applications*, 35, 225 - 249, 1999.

Wang G, Stone K and Vanka SP, Unsteady heat transfer in baffled channels, *Journal of Heat Transfer - Transactions of the ASME*, 118, 585 - 591, 1996.

Zienkiewicz OC and Taylor RL, *The finite element method*. Vol1. The basis, Fifth Edition, Butterworth and Heineaman, London, 2000.

Zienkiewicz OC, Taylor RL and Nithiarasu P, *The Finite Element Method for Fluid Dynamics*, Elsevier, 2005.